METAL MESH REINFORCED LONG GLASS FIBER THERMOPLASTICS (M-LFRT) – COMPARISON OF EXPERIMENT AND SIMULATION -

N. Voll, A. Meichsner, M. Maier
Institut für Verbundwerkstoffe GmbH
Erwin-Schrödinger-Straße 58; 67663 Kaiserslautern; Germany
Nikolai.voll@ivw.uni-kl.de

SUMMARY

Metallic strengthening structures were embedded in LFRT to improve this material for crash applications. This composite combines positive properties of both components and guarantees structural integrity during crash. To enhance the understanding of failure behavior, numerical simulations were performed and compared with experimental results.

Keywords: crash, structural integrity, metal mesh (M), long glass fiber reinforced thermoplastic (LFRT), micro modeling, simulation

INTRODUCTION

In the automotive industry long glass fiber reinforced thermoplastics (LFRT) have been implemented in many application areas. This group of materials consists mostly of polypropylene (PP) which is reinforced by long glass fibers (LGF). The main argument for the use of LFRT is the advantageous cost-benefit ratio. Beside their low density and low material costs, LFRT have an advantageous material behavior regarding their processability and recyclability [1]. Despite of all their good properties LFRT show a disadvantageous crash behavior. Due to brittle fracture of LFRT the energy absorption during crash or impact is low. After reaching their dynamic impact strength LFRT tend to a total loss of structural integrity. Therefore, LFRT are primarily used for casings and coverings but not for load carrying or crash relevant parts. With increasing glass fiber (GF) length mechanical properties like tensile modulus, strength and impact resistance also increase [2] yet the use of LGF can improve these properties only to a certain level. Structural integrity after failure remains problematic. To advance the structural integrity it is possible to reinforce the LFRT composite by a third component with ductile behavior, e.g. steel or aluminum alloys. Thus it should become possible to combine the good properties of both materials in one composite. In a manufacturing and material science project, metallic (M) strengthening structures were embedded into LFRT [3]. Main objective of the research on metal reinforced LFRT (M-LFRT) was to improve the structural integrity of the novel composite after failure of the LFRT compared to neat LFRT. Independent research on a steel cord reinforced glass mat reinforced thermoplastic (GMT) bumper beam [4] and woven steel reinforced Polypropylene [5] have demonstrated that the resulting composites can combine the positive properties of

metals and fiber reinforced thermoplastics. Therefore, a manufacturing process on laboratory scale was developed in a research project at the Institut für Verbundwerkstoffe GmbH in Kaiserslautern/Germany.

MANUFACTURING

The manufacturing process consists of two manufacturing steps. At first semi-finished LFRT plates are produced in a discontinuous compression molding process (see fig. 1).

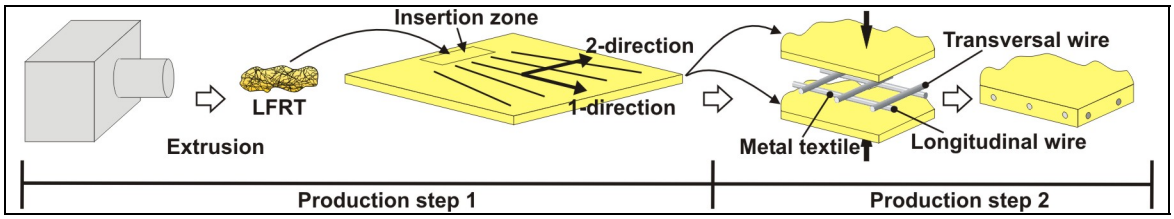

Figure 1: Manufacturing process LFRT plates and M-LFRT

Because of the excentric insertion zone of the extrudate all of the inserted LFRT flows in the same direction during the compression molding process. Due to this unidirectional flow LGF have a preferred orientation in 1-direction (see [3], [6], [7]). In the second production step the semi-finished plates are stacked together with the desired high-grade steel (X5CrNi1810) textile reinforcement as shown in fig. 1. The stack was then heated and inserted in the mold of a hydraulic and parallel controlled press. After cooling down the press was opened and the finished M-LFRT was extracted. In former studies several different production parameters, reinforcement textiles and GF contents were researched in order to get a M-LFRT composite with high energy absorption during crash or impact [3], [8]. Under several loading conditions a spot welded grid (SG) reinforced LFRT40 (40 weight-% LGF) showed good energy absorption properties in combination with maintaining its structural integrity after failure of the LFRT [9]. SG is not produced in a weaving process like classical fabrics. It consists of longitudinal and transversal wires, which are spot-welded at each crossing point (see metal textile in fig. 1). The metal reinforcement had a grammage of 1.8 kg/m^2 and led to an increase of density from 1.2 kg/dm³ to 1.8 kg/dm³ for the metal reinforced composite.

EXPERIMENTAL CHARACTERIZATION

To improve the understanding of the failure behavior of M-LFRT a large variety of experimental tests were carried out. Due to the preferred orientation of the GF, experimental tests were performed in several loading directions. With these tests mechanical properties of the new created SG-LFRT were investigated and compared with unreinforced LFRT. By means of impact and bending/tension tests the favored improved structural integrity of SG-LFRT was tested. Due to the light weight construction application the density specific properties are also to be considered. Density specific values were calculated by dividing tensile modulus, strength, shear modulus and shear strength values by the particular material density.

Tension Properties

Tension tests were performed referring to standard [10]. In the beginning the absolute tensile modulus in 1- (LFRT-1 and SG/LFRT-1) and 2-direction (LFRT-2 and SG/LFRT-2) was determined. The results are shown in fig. 2. The absolute tensile modulus of LFRT has been significantly improved by the spot welded steel grid reinforcement. This applies especially in 2-direction. The increase of density by a factor of 1.5 caused by the metal textile results in a less protruding improvement of the specific tensile modulus. The LFRT-fracture-stress in 1-direction was decreased by the metallic reinforcement. A contrary behavior occurs under tension in 2-direction. The tensile strength of SG/LFRT in 2-direction is higher than without textile reinforcement. Compared to unreinforced LFRT the weight specific tensile strength of textile reinforcement LFRT is less than the absolute values in both directions. The high density and relatively low absolute strength of novel SG-LFRT-composite are responsible for this decline.

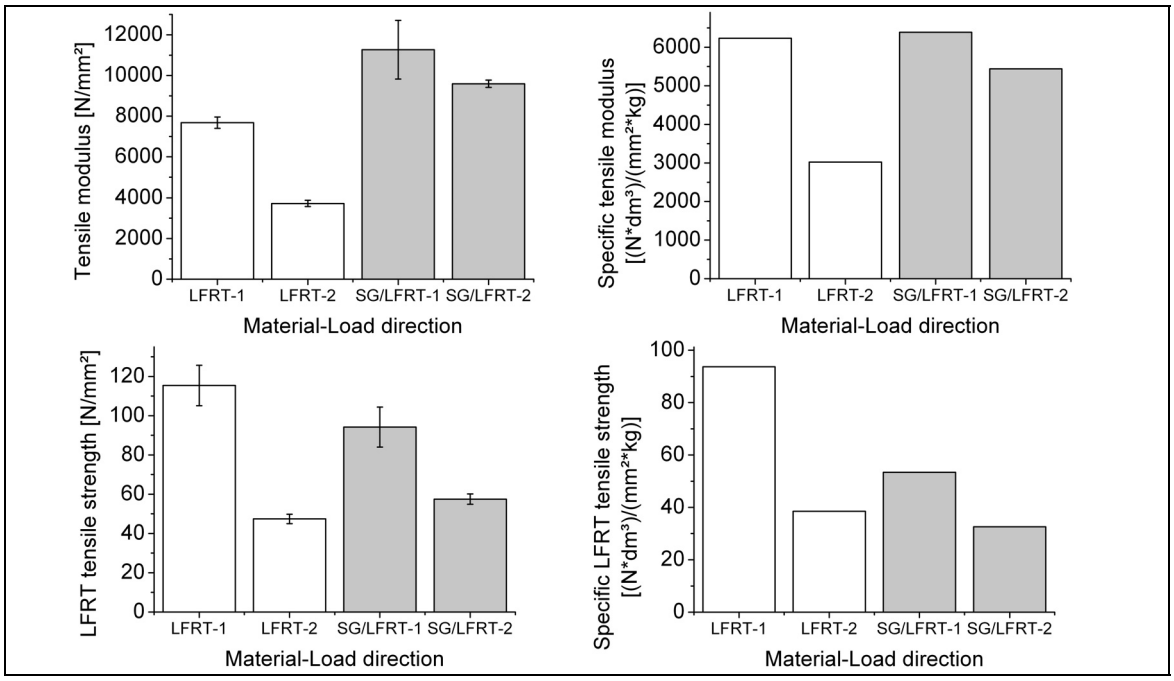

Figure 2: Tensile modulus and strength of LFRT and M-LFRT in 1- and 2-direction

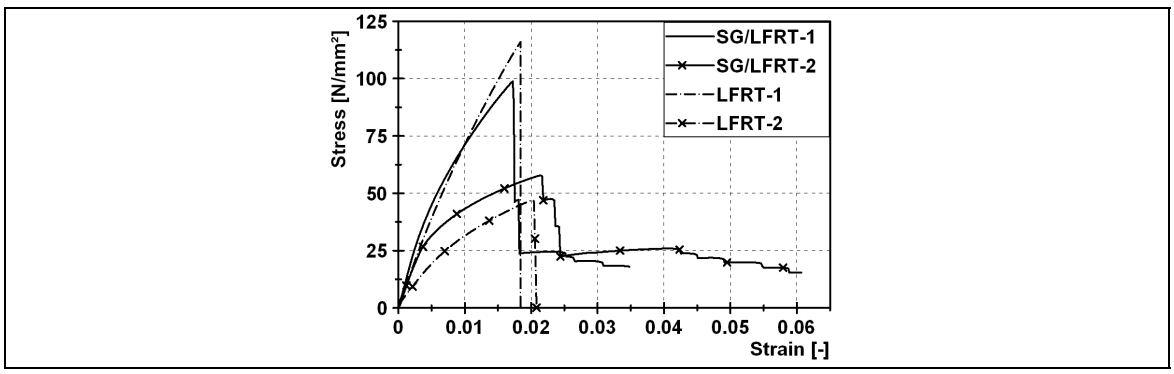

Figure 3: Tensile stress vs. strain of SG/LFRT and LFRT

In fig. 3 the averaged tension behavior of LFRT and SG/LFRT is illustrated. After failure of brittle LFRT at about 1.7 % the tension stress drops. After fracture of the LFRT the ductile metal textile resumes the load transmission. The fracture always appears at a transversal wire. The adjacent transversal wires act as anchors.

Shear Properties

According to [11], the assumption of orthotropic behavior can be proven by means of quasi static shear tests. Therefore, shear properties were investigated in 12- and 21-direction referring to [12]. Test results provided evidence of orthotropic behavior for the LFRT as well as the SG-LFRT. Consequently, only properties in 12-direction are shown in the following figures. In fig. 4 the averaged shear modulus of neat LFRT and SG-LFRT in 12-direction is shown.

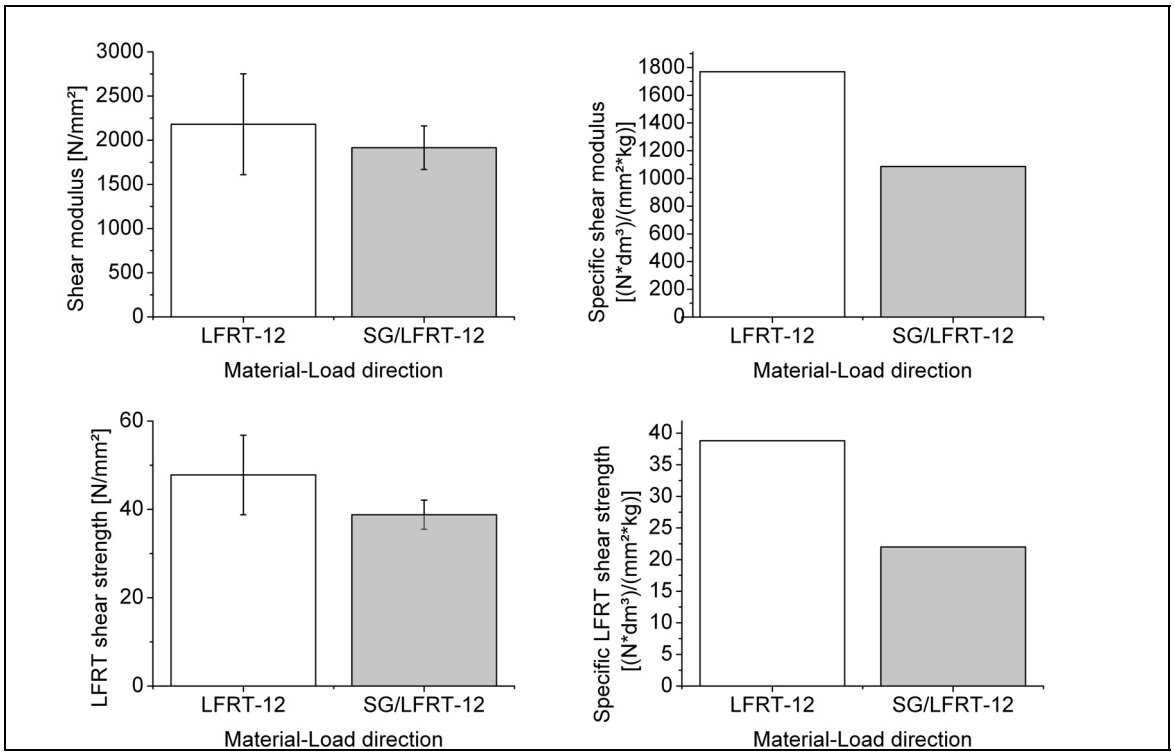

Figure 4: Shear modulus and shear strength of SG/LFRT and LFRT

Unlike in the tension tests steel reinforcement leads to a decrease of shear modulus. The reason is the structurally founded low shear modulus of the SG. This becomes visible especially for the specific shear modulus. In fig. 4 the averaged shear stresses at LFRT failure are shown. The results are similar to the modulus properties. Metal textile increases density and destabilizes the LFRT. This results in a decrease of strength, especially for the specific values. In fig. 5 the averaged shear stress-shear strain curves are shown. In spite of the decrease of shear modulus and strength caused by the textile, the overall energy absorption properties and structural integrity of the composite are superior to the unreinforced LFRT. While plain LFRT sustains an abrupt fracture at a shear strain of about 4 %, metal textile reinforcement of SG/LFRT continues load

transmission at a high level. Complete fracture occurs not before a shear strain of approximately 40% is reached.

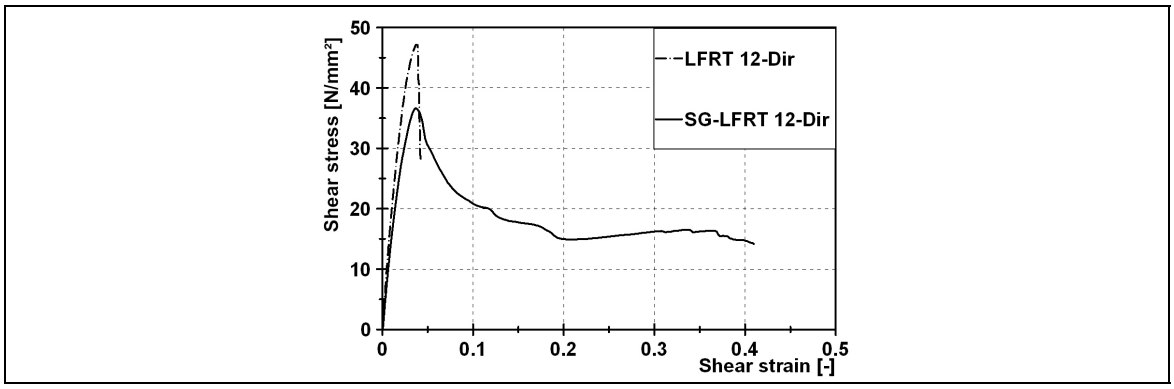

Figure 5: Shear stress vs. shear strain of SG/LFRT and LFRT

Evaluation of Dynamic Energy Absorption of SG-LFRT

The influence of the metal reinforcement on the dynamic energy absorption was investigated with a test following [13]. The functional principle of the impact test is shown in fig. 6 (left). The clamped rectangular specimen is penetrated by the falling dart. The force and deformation signal is recorded during the test and is shown in fig. 6 (right). After numerical integration of the force as function of the deformation the resulting absorbed impact energy was calculated, which is also shown in fig. 6. The specimens were impacted with about 7.8 m/s. For the SG-LFRT a clear increase of the maximum impact force becomes visible compared to LFRT. The absorbed energy reaches nearly triple value.

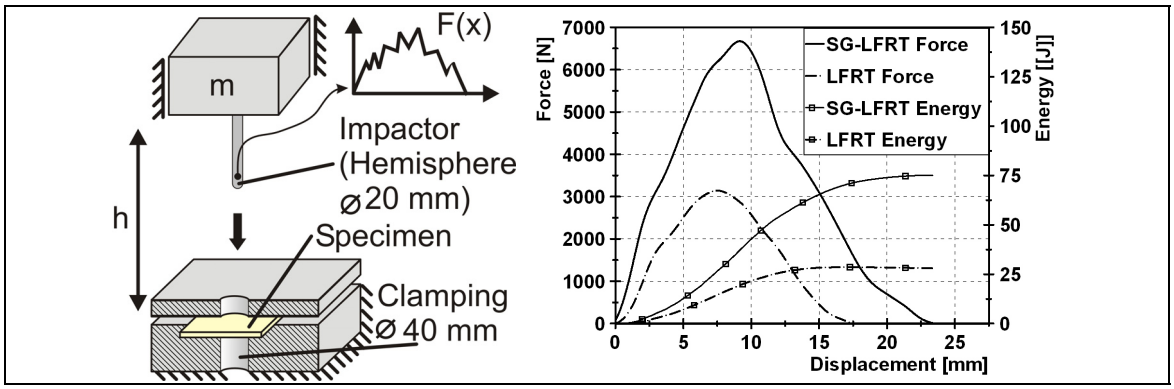

Figure 6: Test set-up and averaged force vs. displacement during impact

Evaluation of Structural Integrity Improvement of SG-LFRT

Due to the new development of SG reinforced LFRT the material is presently not used for industrial applications. Therefore, it becomes necessary to run hypothetical component tests. Simple demonstrator parts were manufactured by thermoforming SG-LFRT stripes to 90 degree angles. These angles were used as inserts for injection

molding and were tested under bending/tension load. It was possible to visualize the improvements in structural integrity of LFRT parts through metallic reinforcement, on the basis of this not standardized quasi static test. Test setup and results are shown in fig. 7. In the beginning of the test bending is dominating. After LFRT fracture at a displacement of about 10 mm the force drops and with increasing displacement the load fades in a pure tension test. At this point the unreinforced LFRT shows just an insignificant residual fracture peak while metal reinforced LFRT reaches its maximum force at a displacement of about 45 mm. The reinforcement of LFRT with SG has a positive influence on strength and energy absorption properties. Additionally, the structural integrity was strongly improved.

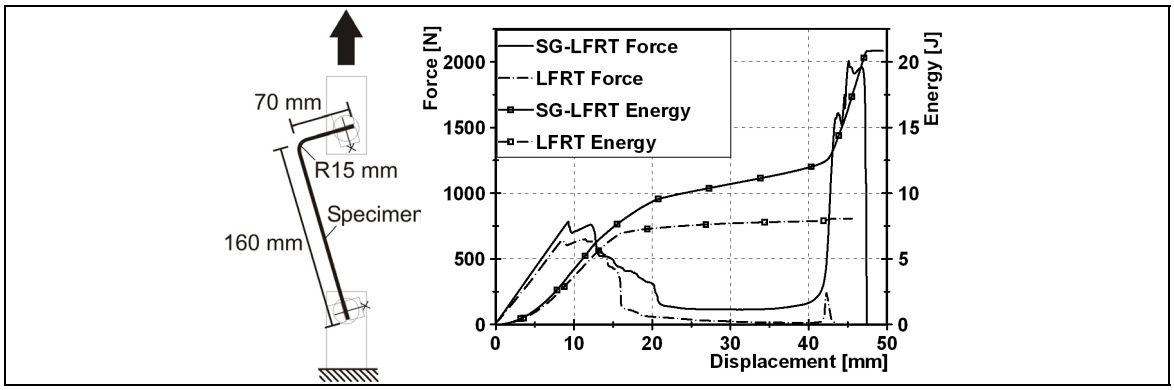

Figure 7: Test setup and averaged force/displacement during angle bending/tension

SIMULATION

To gain a deeper insight into the failure behavior of M-LFRT, than possible with experiments, numerical simulations on micro scale level had to be performed [14] (see fig. 8). For this model LGF and PP were considered as homogenized and only the resulting LFRT and steel textile were modeled. Due to the mesh width of 6 mm and the 1 mm diameter of the metal wire length and width of one unit cell calculates to 3.5 mm. Due to the experimentally observed failure behavior of SG-LFT 6 unit cells (anchor effect of transversal wires) had to be modeled consecutively.

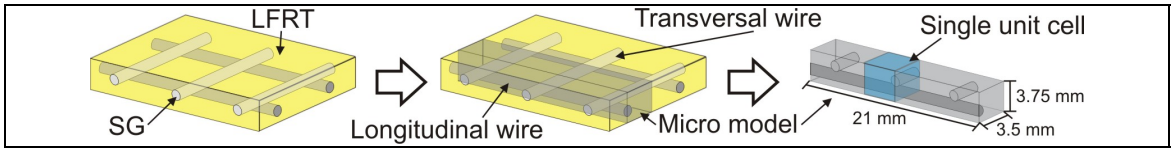

Figure 8: Geometry of the micro model and the unit cell

For the metal phase of the composite a linear elastic material model with plasticity and failure criterion was used. For the LFRT phase of the model an orthotropic linear elastic user defined material model was implemented. Among others, material parameters were taken from the made tension and shear tests. To make simulation results better comparable with experimental data, the remaining of the experimentally investigated 150 mm long samples was modeled with a curve fitting material model, using the

experimentally investigated stress strain values of the composite. Due to the preferred direction of the GF in 1-direction transversely isotropic behavior was assumed, with direction 1 as the principle fiber direction. The 2- and 3-direction are aligned in the plane of isotropy [15], [16]. To allow LFRT to craze locally the user-defined material was advanced by a perfect plastic behavior after reaching the maximum stress criterion. According to [17], the maximum stress criterion compares better to experimental results. For failure, a simple maximum strain criterion was implemented. To investigate the influence of the interface between metal and LFRT one simulation was run without adhesion between metal and LFRT, and one with perfect adhesion.

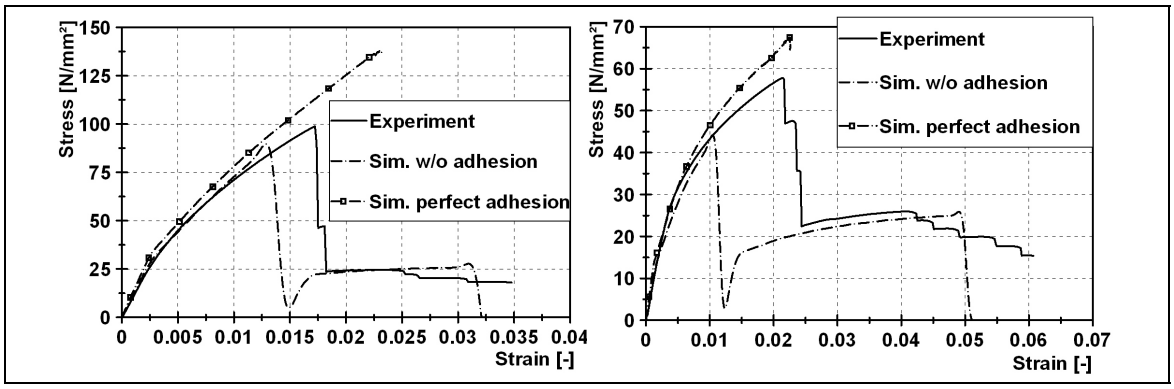

Figure 9: Simulation results in 1- (left) and 2-direction (right)

The simulation results are shown in fig. 9. Very good correlation exists especially in the beginning of the simulation. The experimental curve lay between no and perfect adhesion results in 1- and 2-direction. The model delivers a good prediction of the steel wire rupture towards the end of the test. As in the experimental tests the steel wire ruptures not at intersection points but in-between (see fig. 10). Visual analysis shows that the transversal wires lead to a strong internal notch effect which causes the experimental made observation of recurrent LFRT fracture at the transversal wires. For this reason unreinforced LFRT reaches higher strength and shear strength values. The simulation result reveals room for improvement by an advancement of adhesion between LFRT and metal textile.

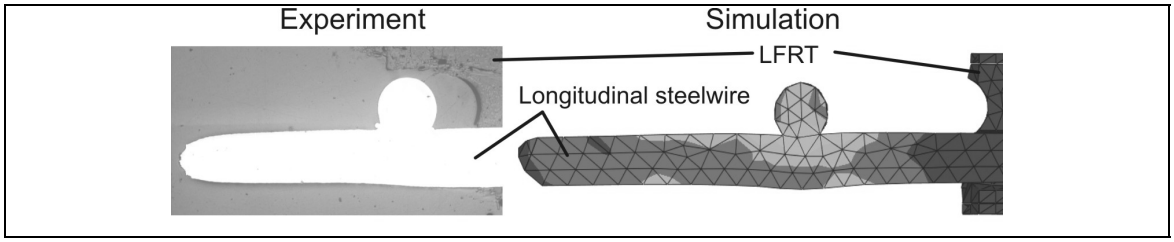

Figure 10: Comparison of simulation and polished cut image (after SG rupture)

The negative influence of the transversal wires (notch effect) was minimized and the fracture strength of the composite was increased to values exceeding the strength of plain LFRT. Fig. 11 shows a comparison of simulation results and a polished cut image.

Due to the notch effect, crazing occurs directly above the transversal wires (I). Analogue to experimental crazing, in the simulation the material model reaches the maximum stress criterion (perfect plastic behavior) in this area (III). The predicted anchor effect was also being confirmed (II & IV).

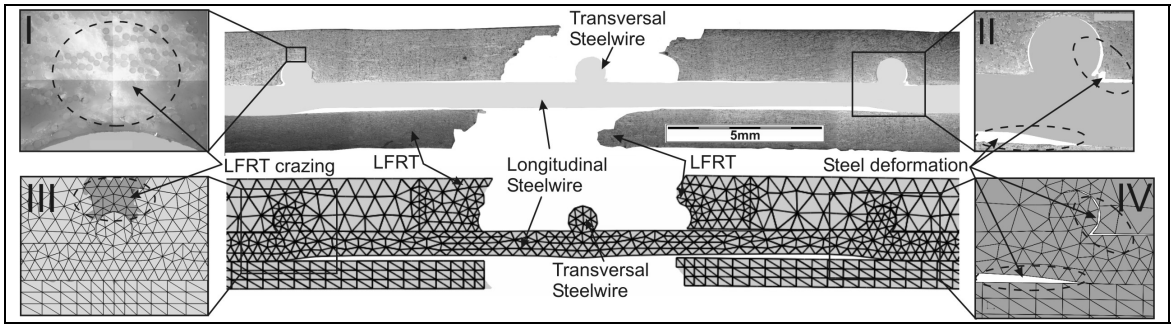

Figure 11: Comparison of simulation and polished cut image (After LFRT rupture)

Optical strain measurement data was compared with simulation results. Even though a simplified material model for LFRT was used the comparison of simulation and experimental data shows matching strain values near the embedded metal wires (see fig. 12) of 0.6-0.73 % as well as 1.8-2.8 %. The deflection of strain position results most likely in the made model simplifications.

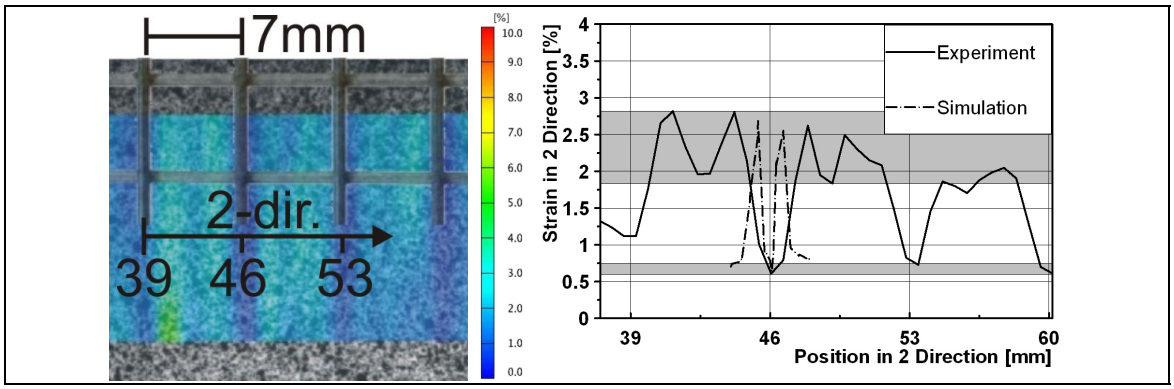

Figure 12: Comparison of experimental and simulative strain measurement

OUTLOOK

The next step is to validate the micro model with more complex load cases. Simulation results of impact and penetration tests will be compared with experimental results. Fig. 13 (right) shows first simulation results of a dynamic impact test. After a good correlation of simulation and experiment in the beginning, large differences occur during progression of the simulation (left). This deflection is caused by the complex failure behavior of LFRT. On the one hand the model does not consider strain rate sensitivity of LFRT. On the other hand it is not possible to simulate residual GF pull-out after fracture. In the experiment fractured LFRT remains connected to the specimen via residual GF. These remaining LFRT pieces absorb energy during the experiment, while

in the simulation these pieces are getting disconnected from the specimen after failure (middle). The fracture of the metal textile is predicted correctly. While in experimental and simulative results of tension test the wire ruptured between intersection points, the impacted wires of simulation and experiment break predominantly near the intersection points. The welding itself remains intact.

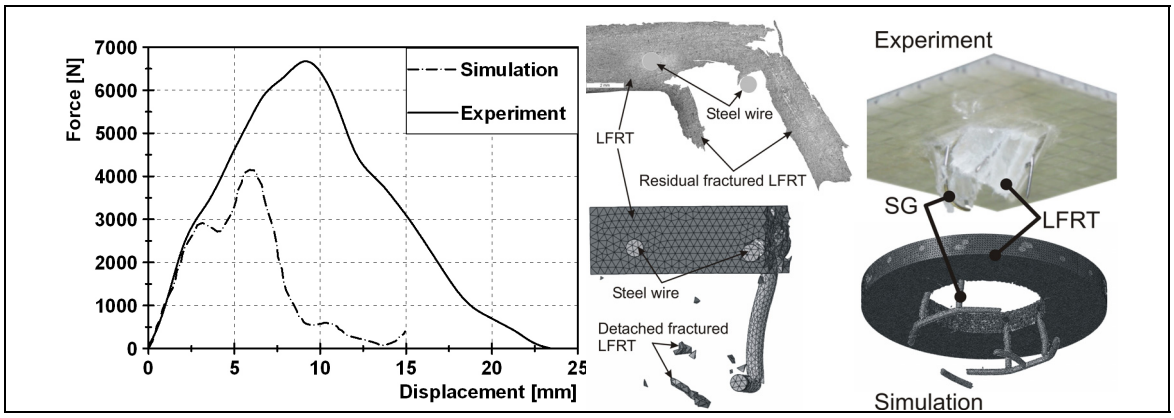

Figure 13: Impact simulation vs. experiment

To investigate the influence of strain rate, dynamic tension tests, and static penetration tests will be performed in the future. The model was programmed as a parametric model in python script. With this ability, parametric simulations will be made to investigate the influence of mesh width, wire thickness, and other parameters. Parallel to this work a user-defined material model will be programmed to simulate the behavior of SG-LFRT.

ACKNOWLEDGEMENTS

The authors thank the “Deutsche Forschungsgemeinschaft (DFG)” for their support of the research project within the scope of the graduate school 814-2 „Ingenieurmaterialien auf verschiedenen Skalen: Experiment, Modellierung und Simulation“.

References

1. Schemme, M.: Verfahrens- und Anwendungstechnik langfaserverstärkter Thermoplaste (LFT). Langfaserverstärkte Thermoplaste in der Automobilindustrie, 2004, Würzburg, Germany.
2. Schemme, M.: Long glass fiber thermoplastics - Material classification and characterization. 2001, s.l..
3. Meichsner, A.; Maier, M.: Optimierung des Herstellungsprozesses von metallfaserverstärkten Kunststoffen (MFK) – mechanische Eigenschaften und Struktur. Technomer Chemnitz, 2007, Germany.
4. van Koert, K.; Durie, A.; Opperman, H.; et al.: An upgraded GMT-Material for energy absorbing structures. 11th International AVK Conference, 2008, Essen, Germany.

5. Erkendirci, Ö., F.; Avci, A.; Akdemir, A.: Fatigue and Fracture Behavior of Woven Steel Reinforced Polyethylene Composite. Journal of Reinforced Plastics and Composites: 27, 2008, p. 1545–1557.

6. Radtke, A.; Henning, F.; Eyerer, P.: Modellierung und Charakterisierung von LFT-D-Strukturen mit lokalen Verstärkungen. Fraunhofer Institut für Chemische Technologie, 2003, Baden-Baden.

7. Reichhold, J.; Rüegg, A.; Schijve, W.: Long Fiber Thermoplastic Materials (LFT) – Material properties properly characterized. 10th International AVK Conference, 2007, Stuttgart.

8. Meichsner, A.; Voll, N.; Maier, M.: Experimentelle und numerische Untersuchung des Deformations- und Bruchverhaltens von edelstahltextilverstärkten Kunststoffen und LFT-Werkstoffen. Journal of Plastics Technology: 5, 2008, p. 48-70.

9. Meichsner, A.; Voll, N.; Maier, M.: Innovative stainless steel fabric – reinforced composites. 11th International AVK Conference, 2008, Essen, Germany.

10. DIN EN ISO 527: Kunststoffe - Bestimmung der Zugeigenschaften. 1996.

11. Krivachy, R.: Charakterisierung und Modellierung kurzfaserverstärkter thermoplastischer Kunststoffe zur numerischen Simulation von Crashvorgängen. Ernst-Mach-Institut, 2007, Freiburg, Germany.

12. ASTM International D 4255/D 4255M-01: Standard Test Method for In-Plane Shear Properties of Polymer Matrix Composite Materials by the Rail Shear Method. 2002.

13. DIN EN ISO 6603: Bestimmung des Durchstoßverhaltens von festen Kunststoffen. 2002.

14. Voll, N.; Meichsner, A.; Maier, M.: Edelstahltextilverstärkte Verbundwerkstoffe - Experiment und Simulation. IVW-Kolloquium, 2008, Kaiserslautern, Germany.

15. Seelig, T.; Latz, A.; Sanwald, S.: Modeling and crash simulation of long-fibre-reinforced thermoplastics. 7. LS-DYNA Anwenderforum, 2008, Bamberg, Germany.

16. Eckardt, J.; Borth, O.; Busch, M.; et al.: An improved characterisation of long-fibre thermoplastics for numerical simulation of components. Polymer Processing Society, 2005, Leipzig, Germany.

17. N.N.: LS-DYNA keyword user's manual 970. 2003, p. 20.179.

Previous Paper **Back to Programme** **Back to Topic**